**Title**
AB INITIO EFFECTIVE CORE POTENTIALS INCLUDING RELATIVISTIC EFFECTS. II. POTENTIAL ENERGY CURVES FOR Xe2>Xe2+> AND Xe2*



**Author**
Ermler, Walter C

**Publication Date**
1978-03-01

Submitted to Journal of Chemical Physics

LBL-7619
Preprint

# AB INITIO EFFECTIVE CORE POTENTIALS INCLUDING RELATIVISTIC EFFECTS. II. POTENTIAL ENERGY CURVES FOR $Xe_2$, $Xe_2^+$, AND $Xe_2^*$

Walter C. Ermler, Yoon S. Lee,
Kenneth S. Pitzer, and Nicholas W. Winter



March 28, 1978

Prepared for the U. S. Department of Energy
under Contract W-7405-ENG-48



LBL-7619

## DISCLAIMER

# AB INITIO EFFECTIVE CORE POTENTIALS INCLUDING RELATIVISTIC EFFECTS. II. POTENTIAL ENERGY CURVES FOR $Xe_2$, $Xe_2^+$, and $Xe_2^*$ †

Walter C. Ermler, Yoon S. Lee, and Kenneth S. Pitzer

Department of Chemistry and Lawrence Berkeley Laboratory
University of California, Berkeley, CA 94720

and

Nicholas W. Winter

Theoretical Atomic and Molecular Physics Group
Lawrence Livermore Laboratory
Livermore, CA 94550

† This work was performed under the auspices of the U. S. Department of Energy under Contract No. W-7405-ENG-48.

## Abstract

Potential energy curves for the ground $^1\Sigma_g^+$ state of $Xe_2$, the first four states of the $Xe_2^+$ ions, and the eight $Xe_2^*$ excimer states corresponding to the addition of a $6s\sigma_g$ Rydberg electron to these ion cores have been computed using averaged relativistic effective core potentials (AREP) and the self-consistent field approximation for the valence electrons. The calculations were carried out using the LS-coupling scheme with the effects of spin-orbit coupling included in the resulting potential energy curves using an empirical procedure.

A comparison of non-relativistic and averaged relativistic EP's and subsequent molecular calculations indicates that relativistic effects arising from the mass-velocity and Darwin terms are not important for these properties of $Xe_2$ molecules. Spectroscopic constants for $Xe_2^+$ are in good agreement with all electron CI calculations suggesting that the computed values for $Xe_2^*$ excimers should be reliable. The lifetime for the $O_u^+$ state of the $Xe_2^*$ is computed to be 5.6 nsec which is in the range of the experimentally determined values.

## Introduction

Laser oscillation has been observed for each of the rare gases except Ne, and for rare gas mixtures.[1] These lasers make use of the bound-free transition between the excited rare gas dimer (excimer) and the repulsive ground state. The excimer and dimer ion states also play an important role in the kinetics of rare-gas-halide lasers. The kinetic and radiative models designed to describe the fluorescence and coherent emission of these laser systems requires knowledge of radiative lifetimes and cross sections for photoionization, optical absorption, and stimulated emission.

The $Xe_2$ excimer has received considerable attention due to its importance as an intense source of vacuum ultra-violet radiation with applications in laser photochemistry and as a pump for fusion lasers. Extensive theoretical modeling and experimental investigation have given insight into the difficulties of the $Xe_2$ laser, including scaling with pressure, photoionization, and accessing the excimer states with long radiative lifetimes.[2] In order to further refine the modelling of these processes more precise knowledge of the states of $Xe_2$ and $Xe_2^+$ is required.

Previous theoretical studies on the excited states of $Xe_2$ and $Xe_2^+$ are limited to the empirical potential energy curves derived by Mulliken[3,4] and the all electron configuration interaction calculations of Wadt[5] on the ground state of $Xe_2$ and four states of $Xe_2^+$. Concurrent with this work Wadt et al.[6] have carried out further calculations on $Xe_2^+$

using effective core potentials to replace the inner shell electrons. Our results extend quantitative calculations to the excited states of neutral $Xe_2^*$ and provide interesting comparisons of the different methods for the states of the ion $Xe_2^+$.

The calculation of the potential energy curves for the heavier rare gas dimers presents two obvious difficulties. The first is the large number of electrons to be treated (most of which are not directly involved in determining the properties of interest). In addition, relativistic effects such as spin-orbit interactions increase significantly for higher Z. While relativistic effects become much larger for still heavier elements, they are large enough for xenon to make their consideration worthwhile. Recently an approach has been developed[7] to simplify the calculations on heavy atoms by replacing the core electrons with an effective potential that also includes relativistic effects. These potentials are used in the present SCF calculations for $Xe_2$, $Xe_2^+$, and $Xe_2^*$.

These calculations involve several approximations, the most obvious being the SCF approximation. However for other rare gas dimer ions it has been shown that SCF calculations benefit from a fortuitous cancellation of errors and yield good results.[8,9] While the excimer states do not formally dissociate correctly at the Hartree-Fock level, the potential curves should be about as accurate as the ion curves for values of the internuclear distance near the potential minima. Another approximation discussed in more detail in the next

section is the use of LS coupling in the calculations and the inclusion of spin-orbit interaction as a later correction. The next section presents the details of the calculations and the results. The final section is devoted to a discussion of the SCF potential energy curves and radiative lifetimes.

## II. Calculations

All-valence-electron self-consistent-field (SCF) calculations on $Xe_2$, $Xe_2^+$, and $Xe_2^*$ were carried out using Gaussian expansions of effective core potentials (EP) derived[7] using pseudo-orbitals extracted from numerical Dirac-Hartree-Fock atomic wave functions.[10] To make use of existing computer programs based on the LS-coupling scheme for constituent atoms the EP's ($U_{\ell j}^{EP}$) based on the formalism of Ref. 7 are averaged to yield "averaged relativistic effective core potentials (AREP)". Thus each radial component of the total EP is given by

$$U_\ell^{AREP}(r) = \frac{1}{2\ell+1}\,[\ell U_{\ell\ell^-}^{REP}(r)+(\ell+1)\,U_{\ell\ell^+}^{REP}];\ \ell>0,\ \ell^-=\ell-\tfrac{1}{2},\ \ell^+=\ell+\tfrac{1}{2}. \qquad (1)$$

The total EP now is of the form

$$U^{AREP} = U_L^{AREP}(r) + \sum_{\ell=0}^{L-1}\sum_{m=-\ell}^{\ell}[U_\ell^{AREP}(r)-U_L(r)]\ |\ell m><\ell m|, \qquad (2)$$

where $U_L$ is termed the "residual potential" and L is (ideally) one greater than the highest angular momentum occupied in the core. The angular momentum projection operators act on basis functions defined in the LS-coupling reference frame. The EP of Eq (2) may be used in molecular calculations in the same

manner as described by Kahn, Baybut, and Truhlar[11] when expanded in M Gaussian functions as

$$[U_{\ell}^{EP}(r) - Z_c/r] = \sum_{i=1}^{M} b_{\ell i} r^{n_{\ell i}} e^{-\zeta_{\ell i} r^2}, \qquad (3)$$

where $Z_c$ is the number of core electrons.

The EP of Eq (2) includes the effects due to the mass-velocity and Darwin terms in the Dirac Hamiltonian, whereas the spin-orbit effects have been averaged out by virtue of Eq (1). To gauge the magnitude of these effects EP's were derived from non-relativistic numerical Hartree-Fock wave functions[12] following the procedures analogous to those described in Ref 7 for defining the appropriate pseudo-orbitals.

The averaged relativistic EP's (AREP) and the non-relativistic EP's (NREP) are shown in Fig. 1 for $\ell$ = 0, 1, 2. Expansions [Eq. (3)] for the NREP's and AREP's are given in Table I.

A valence basis set of Gaussian-type functions (GTF) was derived by optimization of the valence energy via SCF calculations for the $5s^2 5p^6$ configuration of the Xe atom in the field of the AREP. The orbital exponents of four s-type and three p-type GTF's in a basis set comprised of six s and five p GTF's were optimized while the two functions of each type having the smallest exponents were held fixed at values previously optimized[7] for the 6s and 6p Rydberg orbitals of the Xe atom. The three s and two p GTF's having the largest exponents were contracted together using the atomic SCF orbital coefficients. A single d-type polarization function

that was optimized for the ground state of $Xe_2^+$ was added to yield a final (6s 5p 1d)/[4s 4p 1d] contracted GTF valence basis set. The $\zeta$ values and contraction coefficients are given in Table II. The analogous procedure for the NREP resulted in a basis set that was sufficiently like that due to the AREP that same GTF's were used with both EP's.

The molecular SCF calculations were carried out using the POLYATOM[13] molecular integrals program, the GTF effective potential integrals program of Kahn,[14] and an open-shell SCF program developed at Caltech.[15]

Although EP's for Xe through $\ell$=3 were computed,[7] the present limitation of the EP integral program[14] to symmetries $\ell \leq 2$ required that the residual potential be $U_d^{AREP}(r)$. Earlier investigations have indicated, however, that the EP's for higher $\ell$ have appreciable effects only for cases where basis functions of that symmetry are centered on the same nucleus as the EP.[11] When this is not the case the interaction with EP's of higher $\ell$ comes about only through two- and three-center interactions. Further studies of a proper definition of the residual potential are still warranted because of large differences seen in the shapes of, for example, $U_d^{EP}$ and $U_f^{EP}$ of Xe and $U_f^{EP}$ and $U_g^{EP}$ of Au.[7]

Representative atomic SCF results are given in Table III. Also shown are orbital energies from all-electron AHF[12] and DHF[10] calculations, where the $5p_{1/2}$ and $5p_{3/2}$ orbital energies have been averaged as in Eq (1). Results[6] based on the Cowan and Griffin (CG) approximation,[16] whereby the mass-velocity and Darwin terms are included in the atomic Hamiltonian and

LS-coupling is retained by excluding the spin-orbit term, are also shown. The excellent agreement between the averaged DHF and CG results indicates that for Xe the shift of the 5s orbital energy is nearly independent of the presence of spin-orbit coupling operators. It may also be concluded that the 5p orbital is not radically changed by the presence of the mass-velocity and Darwin terms. This is also reflected in the small difference in the ionization potentials as computed with the AREP and NREP.

SCF calculations using the basis set of Table II and the NREP and AREP of Table I were carried out for the ground $^1\Sigma_g^+$ state of $Xe_2$ and the ground $^2\Sigma_u^+$ state of $Xe_2^+$. The results are plotted in Figs. 2 and 3 together with curves due to all-electron calculations using a contracted Gaussian basis set by Wadt.[5] Also shown in Fig. 2 is a curve based on the electron-gas-model of Gordon and Kim and Rae[17] that was reported by Wadt.[5]

Based on the atomic results of Table III and the near indistinguishability of the AREP and NREP results shown in Figs. 2 and 3 we conclude that for diatomic Xe molecules the relativistic effects due to mass-velocity and Darwin type terms are unimportant. The AREP curves are only slightly displaced to the left of the NREP curves. This is traceable mainly to the contraction of the 5s orbital in the AREP calculation.

Table IV lists the valence energies for the ground state of $Xe_2$ ($1\sigma_g^2\ 1\sigma_u^2\ 2\sigma_g^2\ \pi_u^4\ \pi_g^4\ 2\sigma_u^2$), the four states of $Xe_2^+$

that arise when an electron is removed from each of the outer molecular orbitals (MO), and the eight states of $Xe_2^*$ due to the addition of an electron into the $\sigma_g 6s$ MO relative to each of the four ion cores. Valence energies at 13 internuclear distances for each of the 13 states were computed in separate SCF calculations using the AREP of Table I and the valence GTF basis set of Table II. The $Xe_2^+$ potential energy curves based on these data are shown in Fig. 4 and those for $Xe_2^*$ in Fig. 5.

Spin-orbit coupling effects were approximated for the $Xe_2^+$ and $Xe_2^*$ curves using the empirical model described by Cohen and Schneider.[18] In this procedure the experimental splittings of the $Xe^+$ and $Xe^*$ are used to determine the matrix elements of the spin-orbit Hamiltonian. This matrix is added to the diagonal matrix of energies of the states that interact to yield a given total angular momentum $\Omega$; viz $^2\Sigma^+$ and $^2\Pi$ for $\Omega = 1/2$, $^3\Pi$ and $^1\Sigma^+$ for $\Omega = 0^+$, $^3\Pi$ and $^3\Sigma^+$ for $0^-$, and $^3\Pi$, $^3\Sigma^+$, and $^1\Pi$ for $\Omega = 1$.

Spin-orbit parameters $\zeta$ for $Xe^+$ ($5p^5$) and $Xe^*$ ($5p^5 6s$), derived from the atomic tables of Moore,[19] are $1/3[J(1/2)-J(3/2)] = 3512\ cm^{-1}$ and $2/3[J(0)-J(2)] = 6086\ cm^{-1}$, respectively. These parameters were used to calculate the energy for the $\omega$-$\omega$ coupling case[3] at each internuclear distance for the data in Table IV. The 23 resulting states are plotted and labeled in Fig. 6, where we have shifted the $Xe_2^+$ curves vertically such that the experimental (rather than the SCF) ionization potentials of the Xe atom are reproduced. No adjustments were made in the $Xe_2^*$ curves. Because the

resolution of many of the curves in Fig. 6 is rather poor, the states of $Xe_2^+$ are plotted separately in Fig. 7, and the states of $Xe_2^*$ in Fig. 8.

Values of selected spectroscopic constants for the (strongly) bound $Xe_2^+$ and $Xe_2^*$ states are given in Table V for the curves both with and without spin-orbit coupling. Results based on the all-electron $Xe_2^+$ calculation by Wadt[5] and those due to the use of a relativistic EP[6] for Xe derived from[20] the Cowan and Griffin[16] atomic formalism are also given in Table V for comparison. Some vertical transition energies for $Xe_2^+$ and $Xe_2^*$ are listed in Table VI.

## III. Discussion

Although it has been shown that the relativistic effects other than spin-orbit coupling are not important for the properties calculated here for $Xe_2$, some discussion of the differences between the all-electron calculations of Wadt and the results using the EP's is necessary. It is seen in Figs. 2 and 3 that the EP curves are displaced to the left of the all-electron curves. Presumably the curves from all-electron calculations are more nearly correct, although the limited basis set used for the core electrons in these particular calculations may yield curves that are too repulsive at short distances. Other calculations with effective potentials have yielded curves which also appear to be not repulsive enough.[6,21] Further studies are needed to determine the extent to which this is a difficulty inherent in the effective core potential method as presently employed or to

which it may arise from numerical approximations in the use of basis functions to represent EP's or in other steps in the calculations. The choice of the residual potential $U_L$ (see above) may also contribute to discrepancies. We hope to be able to offer more definite conclusions in the near future.

Finally it is noted that the results using the electron gas approximation[17] are in close agreement with the EP results as shown in Fig. 2. This may be related to the inherent frozen core approximation in the electron gas methods.

The results for potential energy curves of rare gas dimer ions have been shown to be consistently well represented by the SCF approximation due to the cancellation of errors arising from the following effects.[8,9] The SCF wave functions for homopolar ions formally dissociate to two atoms having a +1/2 charge. This is essentially an orbital relaxation effect and reflects the fact that the orbitals describe averages of a neutral atom and a positive ion. Hence, the total energy at large internuclear distance is higher than the sum of the separate atom and ion SCF energies by an amount designated by Gilbert and Wahl[8] as the "left-right" correlation energy. The additional configurations required to acquire the proper atom plus ion limiting value have been discussed in detail elsewhere.[8,5] This orbital relaxation error is balanced by an error of nearly equal magnitude due to the neglect of correlation energy in the bonding region in the use of the SCF approximation. The fact that the approximation is more serious for $Xe_2^*$ is seen in the results at R = 20 in Table IV.

The use of SCF wave functions for the Rydberg $Xe_2^*$ states should be reasonable since they correspond to the addition of a single $6s\sigma_g$ electron to the respective $Xe_2^+$ cores. However, the dissociation products are not as reasonable as in the case of $Xe_2^+$ since the average of ground and excited Xe orbitals are not as similar as are those for Xe and $Xe^+$. It appears from our calculations that the results for the $Xe_2^*$ states are valid for internuclear distances as large as about 9-10 a.u. as shown in Table IV. Spectroscopic constants for the $Xe_2^*$ states given in Table V are, as expected, close to those for $Xe_2^+$, suggesting that the $Xe_2^*$ states are reasonably described by the SCF calculations.

It is important to note that while the $\sigma_g 6s$ Rydberg orbitals is the lowest in energy, there will be bound excimer states due to excitation to the 6p and 5d ($\sigma$, $\pi$, and $\delta$) Rydberg orbitals.[3,4] These will result in avoided curve crossings traceable to the change in character from $\sigma_g 6s$ to the other Rydberg orbitals. In such cases the use of the empirical spin-orbit coupling procedure is no longer valid since the nature of the excited state changes from $5p^5 6s$ to $5p^5 6p$ or $5p^5 5d$.[18] The present SCF calculations do not, of course, allow for a change of orbital character and may be considered as describing the $\sigma_g 6s$ states unperturbed by the presence of nearby states of the same symmetry. Estimates of the curves for these other $Xe_2^*$ states are given in Refs. 3 and 4.

The inclusion of spin-orbit coupling into the curves shown in Figs. 4 and 5 yields curves (Figs. 7-8) that show trends similar to those reported by Cohen and Schneider[18] for $Ne_2^+$ and $Ne_2^*$ and those of Wadt[5] for $Xe_2^+$. The magnitude of the spin-orbit interaction is considerably greater for Xe than for Ne as noted by the shift from a $^1P$ term and a $^3P$ manifold to the pattern of j-j coupling with the pairs of terms with J = 1,2 (for $5p_{1/2}^2\ 5p_{3/2}^3\ 6s$) and J = 0, 1 (for $5p_{1/2}\ 5p_{3/2}^4\ 6s$).

Dipole transition moments for the $^1\Sigma_u^+ \rightarrow {}^1\Sigma_g^+$ and $^1\Pi_u \rightarrow {}^1\Sigma_g^+$ emissions calculated using the respective SCF wave functions are reported in Table VII for several internuclear distances. The transition moments of the states including spin-orbit coupling are related to these through the eigenvectors of the spin-orbit matrices defining the $0_u^+$ and $1_u$ states;[18b] viz,

$$\mu(0_u^+) = a_1\mu(^1\Sigma_u^+) + a_2\mu(^3\Pi_u)$$

$$\mu(1_u) = b_1\ (^1\Pi_u) + b_2\mu(^3\Sigma_u^+) + b_3\mu(^3\Pi_u).$$

Since the transition moments for the triplet states are identically zero the only coefficients required are $a_1$ and $b_1$ ($a_1$ = 0.9753 and $b_1$ = -0.1375 for R = 5.75 $a_o$). The other low-lying spin-orbit state, $0_u^-$, is strictly forbidden to radiate to the ground state. The resultant values for the transition moments including spin-orbit coupling for R = 5.75 $a_o$ are $\mu(0_u^+)$ = 0.7049 a.u. and $\mu(1_u)$ = 0.1297 a.u. The radiative lifetime $\tau$ for a bound-continuum emission can, to a good

approximation, be expressed in terms of the vertical energy between the two states $\Delta E(eV)$ and the transition moment $\mu(a.u.)$ near $R_e$ using the expression $A = \tau^{-1} = 1.063 \times 10^6 |\Delta E|^3 |\mu|^2$ sec for the Einstein coefficient of spontaneous emission.[22] Using the SCF values $\Delta E(O_g^+ - O_u^+) = 6.987$ eV and $\Delta E(O_g^+ - 1_u) = 6.878$ eV the computed lifetimes are $\tau(O_u^+) = 5.55$ nsec and $\tau(1_u) = 172$ nsec. These lifetimes have proven difficult to measure experimentally[23-29] because the fluorescence from the low-lying vibrational levels of these two states overlap strongly producing a single broad band at 1720 Å. The experiments are further complicated by electron and heavy particle collisions mixing the $O_u^+$, $O_u^-$, and $1_u$ states and making it very difficult to isolate the population in a single state.[29] Measurements by Keto et al.[24,29] are close to the values used in the kinetic model for the $Xe_2$ laser.[2] They obtained $\tau(O_u^+) = 6.22 \pm 0.8$ nsec and $\tau(1_u) = 100 \pm 2$ nsec. Recent measurements by Shirley and associates[23] using pulsed synchrotron radiation to avoid electron collisions and to excite a specific electronic state of the Xe atom have obtained results tentatively interpreted as yielding similar values. Our calculations also agree generally with those of Keto et al.;[24,29] however more accurate calculations that take into account (1) configuration mixing, (2) proper valence-core orthogonality conditions,[30] and (3) the inclusion of Franck-Condon factors and the continuum contributions in the A coefficient need to be carried out.

The variation of the transition moments with respect to changes in internuclear distance (see Table VII) are not large as would be expected for these Rydberg states. Because the

SCF wave functions do not have the flexibility to allow for proper dissociation, the values at larger separation are expected to be less reliable. The variation of the excitation energy with internuclear distance is expected to have a more significant influence on the lifetime because the emission is to the steep repulsive wall of the ground state potential energy curve.

In order to calibrate the molecular lifetimes, calculations were carried out on the $^3P_1$ and $^1P_1$ states of the Xe atom using exactly the same methods to calculate the wave functions and transition moments as were used for the molecular case. The calculated excitation energies are $\Delta E(^1S_0 - {}^3P_1) = 7.316$ eV and $\Delta E(^1S_0 - {}^1P_1) = 8.395$ eV, and the corresponding transition moments are $\mu(^3P_1) = 0.6133$ a.u. and $\mu(^1P_1) = 0.5280$ a.u. These values lead to the lifetimes $\tau(^3P_1) = 6.39$ nsec and $\tau(^1P_1) = 5.70$ nsec. Anderson[31] has determined the lifetimes of these states to be $3.79 \pm 0.12$ nsec and $3.17 \pm 0.19$ nsec, while recent measurements of Matthias et al.[32] yielded $3.5 \pm 0.1$ nsec and $3.4 \pm 0.1$ nsec, respectively.

It would appear that there is considerable discrepancy between theory and experiment. However, the majority of the error can be attributed to the use of the SCF values for the excitation energy. Using the observed[19] values $\Delta E(^1S_0 - {}^3P_1) = 8.436$ eV and $\Delta E(^1S_0 - {}^1P_1) = 9.570$ eV the calculated lifetimes are $\tau(^3P_1) = 4.17$ nsec and $\tau(^1P_1) = 3.85$ nsec, in reasonable agreement with experiment. Since the SCF excitation energies used in the molecular lifetime calculations are close to the observed values (Table VI), the lifetimes are lowered

by only ~10% if the latter energies are used. Finally, it is expected that the calculated lifetime for the $1_u$ state is less reliable than that for the $0_u^+$ state because of potentially large effects on the $^1\Pi_u - {}^1\Sigma_g^+$ transition moment due to the presence of a bound $\Pi_u$ state involving a $d\Pi_g$ Rydberg orbital and coming from the atomic $Xe(5p^5 6p)$ asymptotic state.[4] The $^1\Pi_u$ state employed in the present calculations, restricted to having $Xe(5p^5 6s)$ parentage due to the use of the SCF approximation, is purely repulsive (Fig. 5).

The results presented here are intended to place the low lying $Xe_2^+$ and $Xe_2^*$ potential energy curves on a somewhat more quantitative foundation than the estimates of Mulliken.[3,4] They have also served to demonstrate the reliability of using EP's for molecular calculations involving heavy atoms. It appears that for Xe dimers the incorporation of the effects of spin-orbit coupling by means of an empirical procedure[18] using experimental atomic term splittings is reliable in cases where strong configuration mixing or change in orbital character is not expected. Atomic and molecular lifetimes computed using the respective SCF wave functions and AREP's yield results that are in reasonable agreement with experiment.

In future work we plan to compute potential energy curves for $Xe_2^*$ states including configuration mixing to insure proper dissociation properties and to allow for the interactions among the 6s, 6p, and 5d Rydberg orbitals. The transition moments as a function of internuclear distance will be recomputed and the theoretical emission spectra for $Xe_2^*$ excimers reported.

ACKNOWLEDGEMENT

We thank Drs. W. R. Wadt, P. J. Hay, and L. R. Kahn for helpful discussions and for providing us with their results prior to publication. We are grateful to Dr. M. Yoshimine for his assistance in the transition moment calculations.

REFERENCES

1. (a) N. G. Basov, V. A. Danilychev, Yu. M. Popov, Sov. J. Quantum Electron, 1, 18 (1971).
(b) H. A. Koehler, L. J. Ferderber, D. L. Redhead, and P. J. Ebert, Appl. Phys. Lett. 21, 198 (1972); J. B. Gerardo and A. W. Johnson, IEEE. J. Quantum Electron. 9, 748 (1973).
(c) P. W. Hoff, J. C. Swingle, and C. K. Rhodes, Appl. Phys. Lett. 23, 245 (1973); W. M. Hughes, J. Shannon, and R. Hunter, Appl. Phys. Lett. 24, 488 (1974).
(d) A. W. Johnson and J. B. Gerardo, J. Appl. Phys. 45, 867 (1974).
2. C. W. Werner, E. V. George, P. W. Hoff, and C. K. Rhodes, Appl. Phys. Lett. 25, 235 (1974), ibid. Report UCRL-77412, Lawrence Livermore Laboratory, Livermore, CA, 1975.
3. R. S. Mulliken, J. Chem. Phys. 52, 5170 (1970).
4. R. S. Mulliken, Radiation Res. 59, 357 (1974).
5. W. R. Wadt, J. Chem. Phys. 68, 402 (1978).
6. W. R. Wadt, P. J. Hay, and L. R. Kahn, J. Chem. Phys. (in press).
7. Y. S. Lee, W. C. Ermler, and K. S. Pitzer, J. Chem. Phys. 67, 586 (1977).
8. T. L. Gilbert and A. C. Wahl, J. Chem. Phys. 55, 5247 (1971).
9. W. J. Stevens, M. Gardner, and A. Karo, J. Chem. Phys. (in press).
10. J. P. Desclaux, Computer Phys. Commun. 9, 31 (1975).

11. L. R. Kahn, P. Baybutt, and D. G. Truhlar, J. Chem. Phys. 65, 3826 (1976) and references therein.

12. C. Froese-Fischer, Computer Phys. Commun. 1, 151 (1969); ibid., 4, 107 (1972); ibid., 7, 236 (1974).

13. D. B. Neumann, H. Basch, R. L. Kornegay, L. C. Snyder, J. W. Moskowitz, C. Hornback, and S. P. Liebmann, Program 199, Quantum Chemistry Program Exchange, Indiana University, 1972.

14. L. R. Kahn (private communication).

15. W. J. Hunt, T. H. Dunning, Jr., and W. A. Goddard, III, Chem. Phys. Lett., 3, 606 (1969); W. A. Goddard, III, T. H. Dunning, Jr., and W. J. Hunt, ibid., 4, 231 (1969); W. J. Hunt, W. A. Goddard, III, and T. H. Dunning, Jr. ibid., 6, 147 (1970).

16. R. D. Cowan and D. C. Griffin, J. Opt. Soc. Am., 66, 1010 (1976).

17. R. G. Gordon and Y. S. Kim, J. Chem. Phys. 56, 3123 (1972); A. I. M. Rae, Chem. Phys. Lett. 18, 574 (1973).

18. (a) J. S. Cohen and B. Schneider, J. Chem. Phys. 61, 3230 (1974).

(b) B. Schneider and J. S. Cohen, ibid., 3240 (1974).

19. C. E. Moore, Circ. Nat. Bur. Stand. No. 467, Vol. III (1971).

20. L. R. Kahn, P. J. Hay, and R. D. Cowan, J. Chem. Phys. (in press).

21. P. J. Hay, W. R. Wadt, and L. R. Kahn, J. Chem. Phys. (in press).

22. G. Herzberg, Molecular Spectra and Molecular Structure. I. Spectra of Diatomic Molecules, Van Nostrand Reinhold, Princeton, N.J., 1950. For bound-continuum transitions see F. H. Mies, Mol. Phys. 26, 1233 (1973).

23. D. A. Shirley, private communication.

24. J. W. Keto, R. E. Gleason, Jr., and G. K. Walters, Phys. Rev. Lett. 33, 1365 (1974).

25. A. W. Johnson and J. B. Gerardo, J. Chem. Phys. 59, 1738 (1974).

26. S. C. Wallace, R. T. Hodgson, and R. W. Dreyfus, Appl. Phys. Lett. 23, 672 (1973).

27. D. J. Bradley, M. H. R. Hutchinson, and H. Koester, Opt. Commun. 7, 187 (1973).

28. H. A. Koehler, L. J. Ferderber, D. L. Redhead, and P. J. Ebert, Phys. Rev. A 9, 768 (1973).

29. J. W. Keto, R. E. Gleason, Jr., T. D. Bonifield, G. K. Walters, and F. K. Soley , Chem. Phys. Lett. 42, 125 (1976).

30. R. N. Euwema and L. R. Kahn, J. Chem. Phys. 66, 306 (1977).

31. D. K. Anderson, Phys. Rev. 137, A21 (1965).

32. E. Matthias, R. A. Rosenberg, E. D. Poliakoff, M. G. White, S.-T. Lee, and D. A. Shirley, Chem. Phys. Lett. 52, 239 (1977).

Table I. Gaussian Representations of Xe Effective Core Potentials[a]

| | | NREP | | | AREP[b] | | |
|---|---|---|---|---|---|---|---|
| n | ζ | $b_s$ | $b_p$ | $b_d$ | $b_s$ | $b_p$ | $b_d$ |
| 2 | 3101.0580 | 10001.2468103 | -2029.8635555 | -1261.8724877 | 3364.8358389 | 6400.8867608 | 9715.9126229 |
| 2 | 1656.9400 | 12967.2532014 | -2499.3599334 | -1648.5722662 | 4714.1097300 | 7181.5586116 | 10450.5903027 |
| 2 | 400.1800 | 118.6876949 | 13.6186006 | - 308.8579700 | 408.4806715 | -76.8423330 | -816.3229420 |
| 2 | 213.5110 | -1434.1926222 | 600.2008336 | 2117.2249998 | -1247.2965220 | 76.1691758 | -3178.2001049 |
| 2 | 172.2200 | 1139.0541750 | -75.0987624 | -1683.9676399 | 1181.7588767 | 106.4682087 | 2043.2887265 |
| 2 | 60.1000 | 253.8248434 | 17.1748795 | -1082.1976210 | 357.2926530 | 19.3297540 | 1843.9936166 |
| 2 | 18.0000 | 191.0803909 | 23.5399847 | - 878.3333781 | 279.7260211 | 45.6185250 | 1431.1254621 |
| 2 | 8.7230 | 30.9549072 | 32.9978847 | - 70.6569080 | 24.0259285 | 22.7569696 | 215.1953603 |
| 2 | 5.3170 | -17.6599173 | -41.4064247 | 21.4792185 | 1.6859524 | -31.1191342 | -30.3926954 |
| 2 | 1.4510 | -2.6418222 | -9.3991444 | -5.9585241 | 4.1317641 | -6.6611822 | -4.5418327 |
| 2 | .3000 | -.0320120 | -.0480999 | -.0354254 | -.0318452 | -.0426607 | -.0230183 |
| 2 | .0446 | .0003275 | .0004805 | .0003504 | .0006014 | .0006215 | .0004836 |
| 1 | 7257.5000 | -35.3180702 | -43.4291158 | -37.0120256 | -6.3065139 | 66.8451734 | 101.4665571 |
| 1 | 5425.0000 | 296.9633229 | -14.5635957 | -12.4908299 | 67.9439075 | 65.0477623 | 107.4413732 |
| 1 | 1377.9700 | -335.1700806 | 64.4242171 | 21.2430405 | -122.9570159 | -246.0919993 | -341.0505213 |
| 1 | 185.4100 | 59.0731434 | -35.1381251 | -159.4208658 | 71.5587958 | -4.9626120 | 304.1740320 |
| 1 | 12.9100 | -41.4527070 | -10.2430487 | 152.4005053 | -57.3043753 | -12.1157615 | -358.3400709 |
| 1 | 1.0300 | 9.7418941 | 13.7243283 | 9.3478387 | 4.2814496 | 11.4916197 | 8.9996454 |
| 0 | 165000.0000 | 0.0000000 | -.0800000 | 0.0000000 | 0.0000000 | -.3216667 | -.8080000 |

[a] Relative to Eq. (3). [b] See Eq. (1).

Table II. Xe (6s 5p 1d)/[4s 4p 1d] GTF Basis Set

| Symmetry | Exponent | Coefficient |
|---|---|---|
| s | 28.738697 | -0.015324 |
| s | 1.960972 | -0.192789 |
| s | 0.318521 | 1.099335 |
| s | 0.123316 | 1.0 |
| s | 0.055000 | 1.0 |
| s | 0.021000 | 1.0 |
| p | 2.821521 | 0.084105 |
| p | 0.435800 | 0.964806 |
| p | 0.137219 | 1.0 |
| p | 0.036000 | 1.0 |
| p | 0.013000 | 1.0 |
| d | 0.220000 | 1.0 |

Table III. Xenon Atomic Energies

| State | | Approximation | Orbital Energies (a.u.) 5s | 5p | 6s | ΔE(eV)[a] |
|---|---|---|---|---|---|---|
| Xe $5s^2 5p^6$ | ($^1$S) | DHF(Av) | -1.010 | -0.457 | | |
| | | AHF | -0.944 | -0.457 | | |
| | | NREP | -0.938 | -0.451 | | |
| | | AREP | -1.004 | -0.451 | | |
| | | CG[b] | -1.010 | -0.457 | | |
| $Xe^+$ $5s^2 5p^5$ | ($^2$P) | DHF(Av) | -1.330 | -0.788 | | |
| | | NREP | -1.247 | -0.803 | | 11.203 |
| | | AREP | -1.345 | -0.806 | | 11.187 |
| $Xe^*$ $5s^2 5p^5 6s$ | ($^3$P) | AREP | -1.156 | -0.616 | -0.134 | 7.559 |
| | ($^1$P) | AREP | -1.162 | -0.621 | -0.126 | 7.776 |

[a] Relative to the ground state valence energies E(NREP) = -16.20431 au and E(AREP) = -16.49885 au.

[b] Numerical atomic results using the method of Cowan and Griffin (Ref. 9).

Table IV. Valence SCF Energies of Electronic States of Diatomic Xe[a]

| R | $Xe_2$ | $Xe_2^+$ | | | | $Xe_2^*$ | | | | | | | |
|---|---|---|---|---|---|---|---|---|---|---|---|---|---|
| | $1\Sigma_g^+$ | $2\Sigma_u^+$ | $2\Pi_g$ | $2\Pi_u$ | $2\Sigma_g^+$ | $3\Sigma_u^+$ | $1\Sigma_u^+$ | $3\Pi_g$ | $1\Pi_g$ | $3\Pi_u$ | $1\Pi_u$ | $3\Sigma_g^+$ | $1\Sigma_g^+$ |
| 4.50 | .81444 | .53110 | .42507 | .34045 | .27521 | .64589 | .64179 | .54394 | .53932 | .46150 | .45212 | .32973 | .38823 |
| 5.00 | .90935 | .58558 | .50808 | .45424 | .39509 | .69706 | .69303 | .62280 | .61849 | .57027 | .56233 | .50881 | .50497 |
| 5.50 | .95534 | .60159 | .54494 | .51093 | .46317 | .71099 | .70680 | .65688 | .65272 | .62362 | .61664 | .57446 | .57078 |
| 5.75 | .96839 | .60283 | .55440 | .52742 | .48561 | .71151 | .70718 | .66530 | .66118 | .63888 | .63223 | .59607 | .59227 |
| 6.00 | .97740 | .60176 | .56040 | .53902 | .50286 | .70983 | .70540 | .67044 | .66634 | .64948 | .64309 | .61269 | .60867 |
| 6.25 | .98361 | .59936 | .56409 | .54717 | .51621 | .70712 | .70244 | .67343 | .66934 | .65681 | .65064 | .62560 | .62125 |
| 6.50 | .98789 | .59630 | .56629 | .55290 | .52662 | .70381 | .69893 | .67504 | .67096 | .66189 | .65588 | .63570 | .63098 |
| 7.00 | .99288 | .58972 | .56814 | .55979 | .54124 | .69699 | .69173 | .67598 | .67192 | .66773 | .66206 | .64996 | .64447 |
| 7.50 | .99527 | .58377 | .56844 | .56324 | .55043 | .69099 | .68542 | .67557 | .67155 | .67040 | .66503 | .65894 | .65290 |
| 8.00 | .99643 | .57898 | .56821 | .56499 | .55629 | .68618 | .68040 | .67471 | .67077 | .67148 | .66641 | .66456 | .65835 |
| 9.00 | .99730 | .57271 | .56755 | .56633 | .56252 | .67945 | .67369 | .67264 | .66897 | .67137 | .66694 | .66977 | .66426 |
| 10.00 | .99755 | .56952 | .56711 | .56666 | .56515 | .67486 | .66954 | .67032 | .66701 | .66981 | .66600 | .67056 | .66618 |
| 20.00 | .99703 | .56655 | .56653 | .56653 | .56655 | .64309 | .64067 | .64242 | .64024 | .64241 | .64020 | .64304 | .64098 |

[a] All quantities in a.u. Energies are negative and are relative to -32.00000.

Table V. Spectroscopic Constants for $Xe_2^+$ and $Xe_2^{*a}$

| | | $R_e(a_o)$ | $D_e$(eV) | $\omega_e(cm^{-1})$ | $\omega_e X_e(cm^{-1})$ | $B_e(cm^{-1})$ | $\alpha_e(cm^{-1})$ |
|---|---|---|---|---|---|---|---|
| $Xe_2^+$ $^2\Sigma_u^+$ | This work | 5.74 | 0.99 | 122.5 | 0.45 | 0.02786 | 0.00011 |
| | CI[b] | 6.08 | 1.08 | 124 | | | |
| | CI-EP[c] | 5.84 | 1.04 | 125 | | | |
| $(1/2)_u$[d] | This work | 5.82 | 0.70 | 110.4 | 0.53 | 0.02704 | 0.00013 |
| | CI[a] | 6.18 | 0.79 | 112 | | | |
| | CI-EP[b] | 5.91 | 0.76 | 112 | | | |
| $Xe_2^*$ $^3\Sigma_u^+$ | This work | 5.67 | 1.00 | 128.3 | 0.62 | 0.02856 | 0.00012 |
| $^1\Sigma_u^+$ | This work | 5.65 | 1.03 | 129.2 | 0.45 | 0.02868 | 0.00011 |
| $0_u^+$ | This work | 5.72 | 0.77 | 118.5 | 0.53 | 0.02800 | 0.00013 |
| $0_u^-$ | This work | 5.73 | 0.78 | 117.3 | 0.59 | 0.02793 | 0.00014 |
| $1_u$ | This work | 5.73 | 0.79 | 118.0 | 0.59 | 0.02796 | 0.00014 |

[a] A spin-orbit correction as described in the text was incorporated for the $(1/2)_u$, $0_u^+$, $0_u^-$, and $1_u$ states.

[b] Ref. 5.

[c] Ref. 6.

[d] Empirical estimate of $D_o$ = 1.03 eV, $R_e$ = 6.14 $a_o$ (Ref. 4).

Table VI. Selected $Xe_2^+$ and $Xe_2^*$ Vertical Transition Energies (eV)

| | | This work | CI[a] | CI-EP[b] |
|---|---|---|---|---|
| $Xe_2^+$ | $(1/2)_u \rightarrow (3/2)_g$ | 1.03 | 0.99 | 0.96 |
| | $\rightarrow I(1/2)_g$ | 1.67 | 1.60 | 1.57 |
| | $\rightarrow II(1/2)_g$ | 3.56 | 3.31 | 3.32 |
| $Xe_2^{*c}$ | $O_u^+ \rightarrow XO_g^+$ | 6.99 | | |
| | $1_u \rightarrow XO_g^+$ | 6.82 | | |

[a] Ref. 5.

[b] Ref. 6.

[c] A bound-free emission is observed at 7.3 eV (Ref. 1b).

Table VII. Variation of the Magnitude of the Transition Moment with Internuclear Distance (a.u.)

| State | $^1\Sigma_u^+$ | $^1\Pi_u$ | $0_u^+$ | $1_u$ |
|---|---|---|---|---|
| $R(a_o)$ | | | | |
| 5.5 | 0.691 | 0.953 | 0.678 | 0.115 |
| 5.75 | 0.723 | 0.944 | 0.705 | 0.130 |
| 6.25 | 0.785 | 0.922 | 0.752 | 0.159 |
| 7.5 | 0.901 | 0.866 | 0.804 | 0.207 |
| 8.0 | 0.926 | 0.841 | 0.803 | 0.209 |

## Figure Captions

Fig. 1. Effective Core Potentials of Xe.

Fig. 2. $Xe_2$ $X^1\Sigma_g^+$ Potential Energy Curves. All-electron SCF and electron gas results are taken from Ref. 5.

Fig. 3. $Xe_2^+$ $X^2\Sigma_u^+$ Potential Energy Curves. All-electron POL-CI results are taken from Ref. 5.

Fig. 4. $Xe_2^+$ Potential Energy Curves Without Spin-Orbit Coupling.

Fig. 5. $Xe_2^*$ Potential Energy Curves Without Spin-Orbit Coupling.

Fig. 6. $Xe_2$, $Xe_2^*$, and $Xe_2^+$ Potential Energy Curves Including Spin-Orbit Coupling.

Fig. 7. $Xe_2^+$ Potential Energy Curves Including Spin-Orbit Coupling.

Fig. 8. $Xe_2^*$ Potential Energy Curves Including Spin-Orbit Coupling.

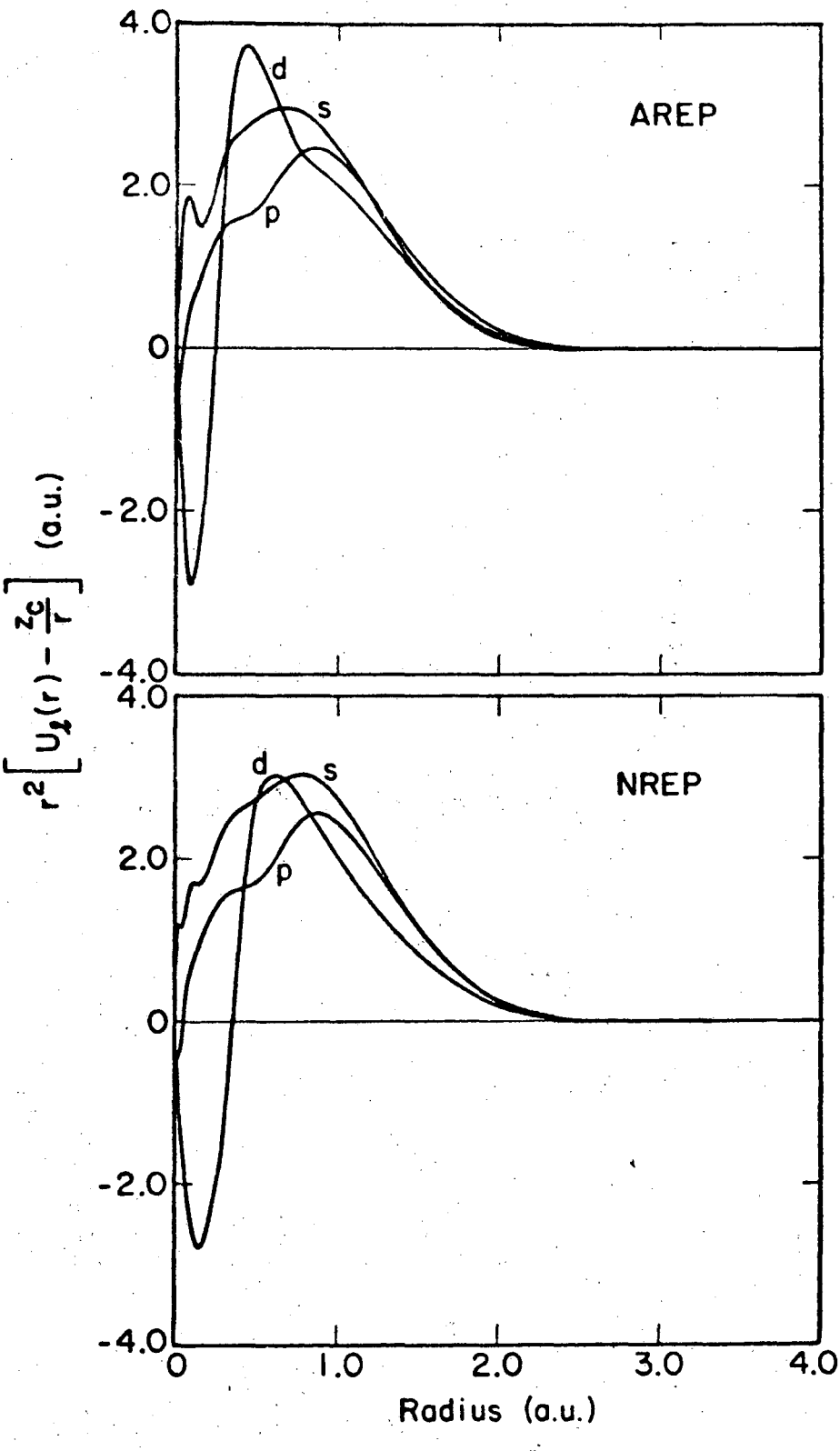
4.0
2.0
0
-2.0
-4.0
d
s
p
AREP
NREP
$r^2\left[U_\ell(r) - \frac{Zc}{r}\right]$ (a.u.)
0
1.0
2.0
3.0
4.0
Radius (a.u.)

Fig. 1

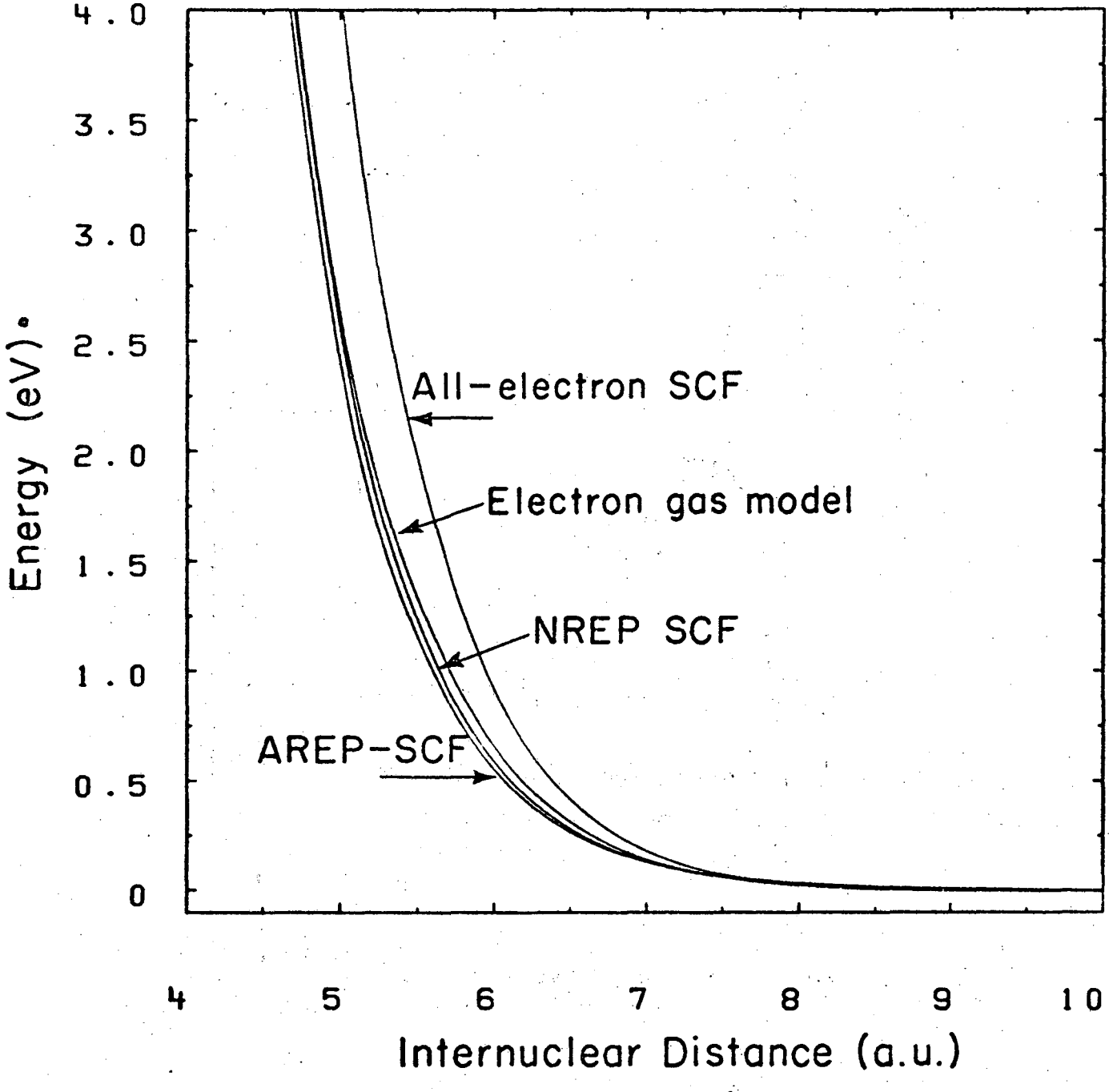
4.0
3.5
3.0
2.5
2.0
1.5
1.0
0.5
0
Energy (eV)
All-electron SCF
Electron gas model
NREP SCF
AREP-SCF
4
5
6
7
8
9
10
Internuclear Distance (a.u.)

Fig. 2

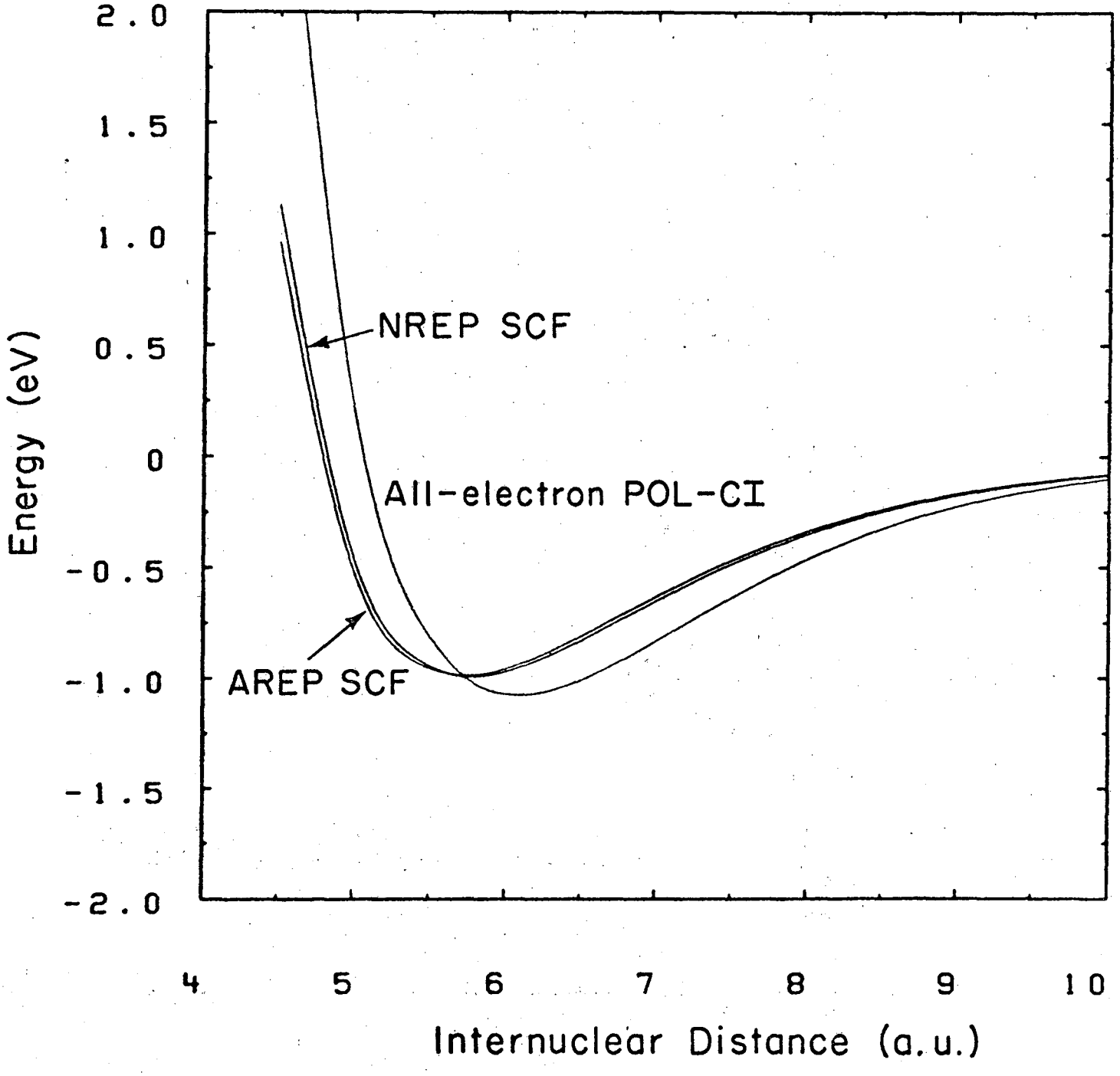
2.0
1.5
1.0
0.5
0
-0.5
-1.0
-1.5
-2.0
Energy (eV)
NREP SCF
All-electron POL-CI
AREP SCF
4
5
6
7
8
9
10
Internuclear Distance (a.u.)

Fig. 3

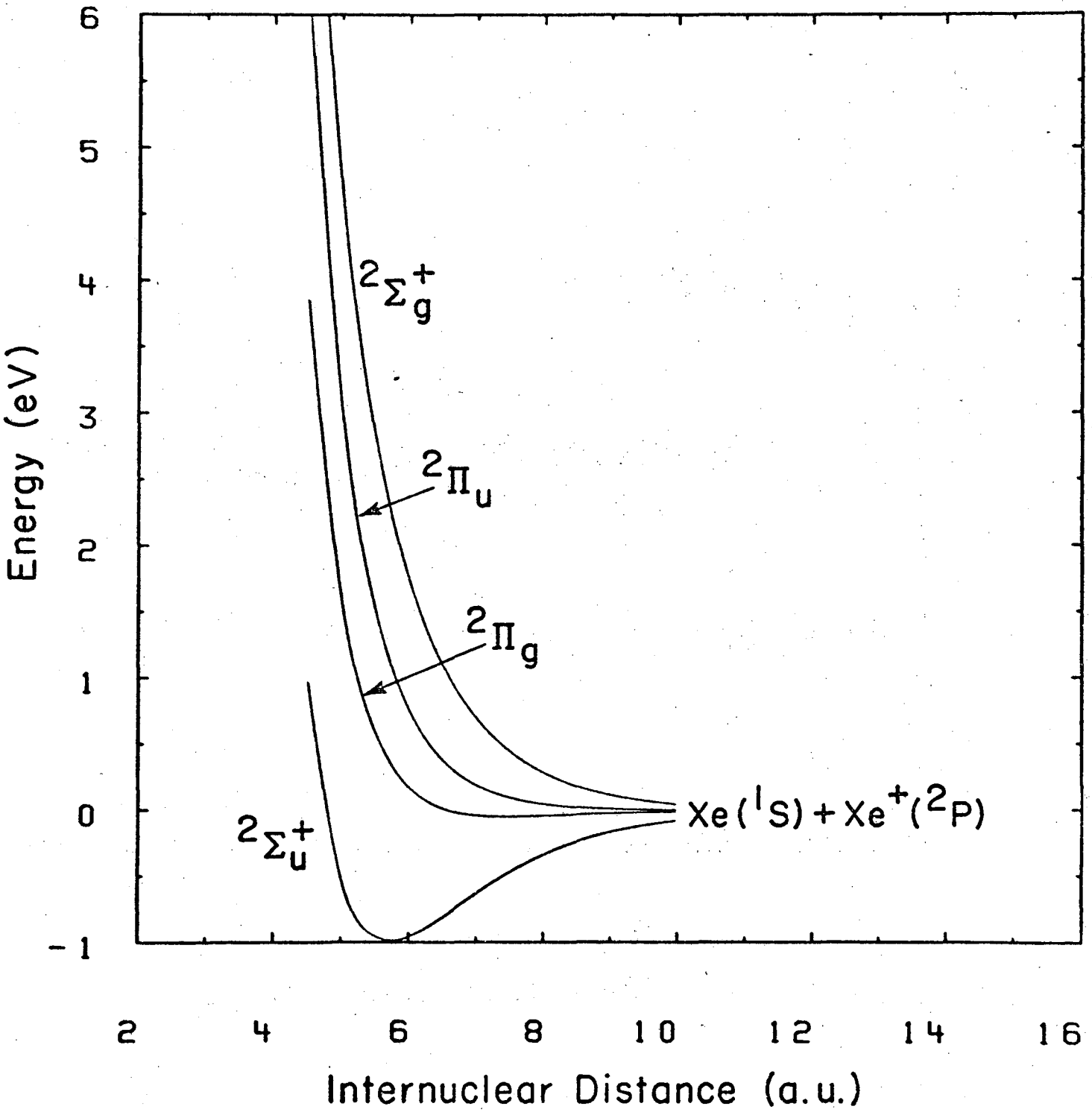
Energy (eV)
6
5
4
3
2
1
0
-1
$^2\Sigma_g^+$
$^2\Pi_u$
$^2\Pi_g$
$^2\Sigma_u^+$
$Xe(^1S) + Xe^+(^2P)$
2
4
6
8
10
12
14
16
Internuclear Distance (a.u.)

Fig. 4

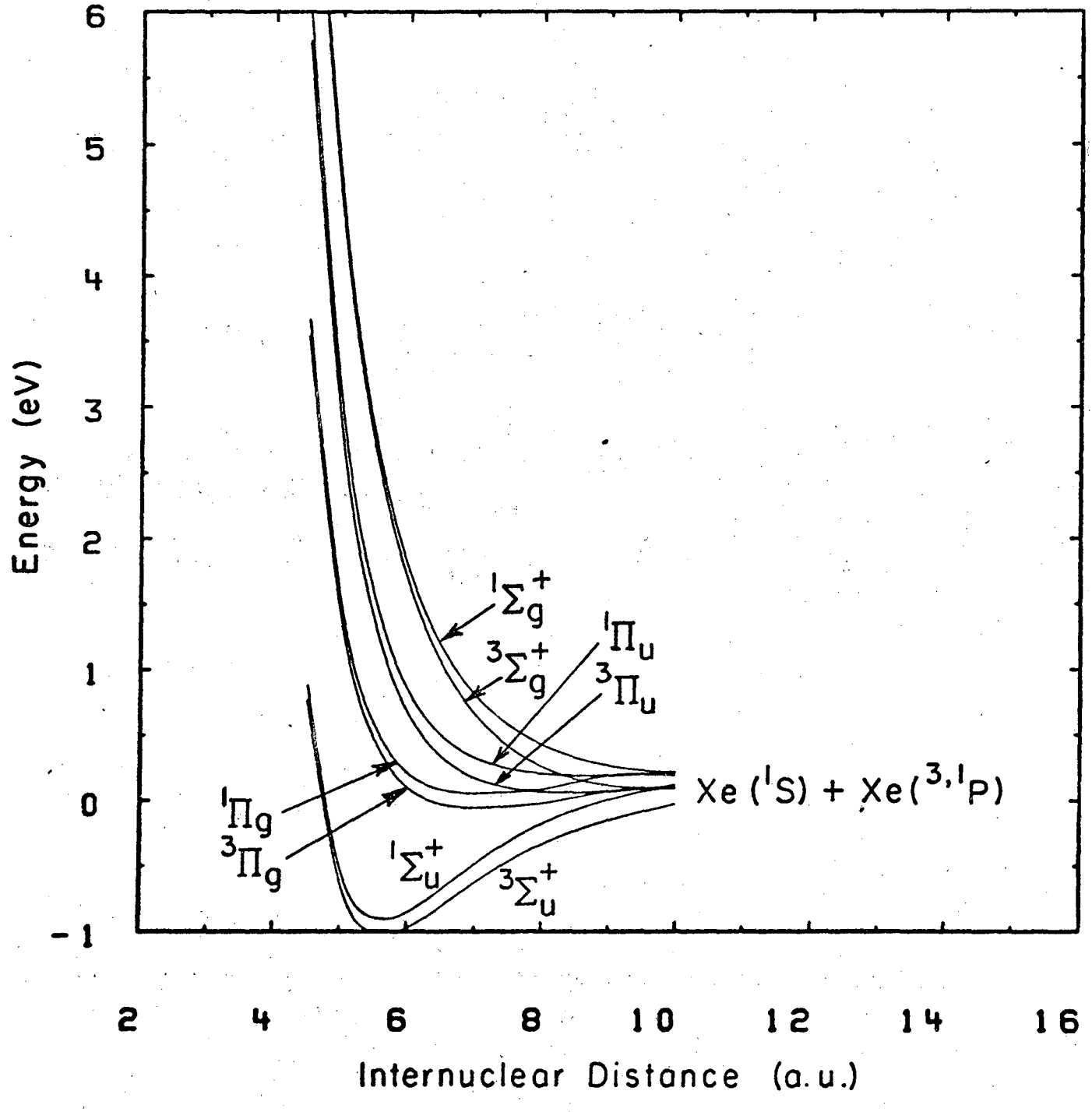
Energy (eV)
6
5
4
3
2
1
0
-1
2
4
6
8
10
12
14
16
Internuclear Distance (a.u.)
$^1\Sigma_g^+$
$^3\Sigma_g^+$
$^1\Pi_u$
$^3\Pi_u$
$^1\Pi_g$
$^3\Pi_g$
$^1\Sigma_u^+$
$^3\Sigma_u^+$
Xe ($^1$S) + Xe($^{3,1}$P)

Fig. 5

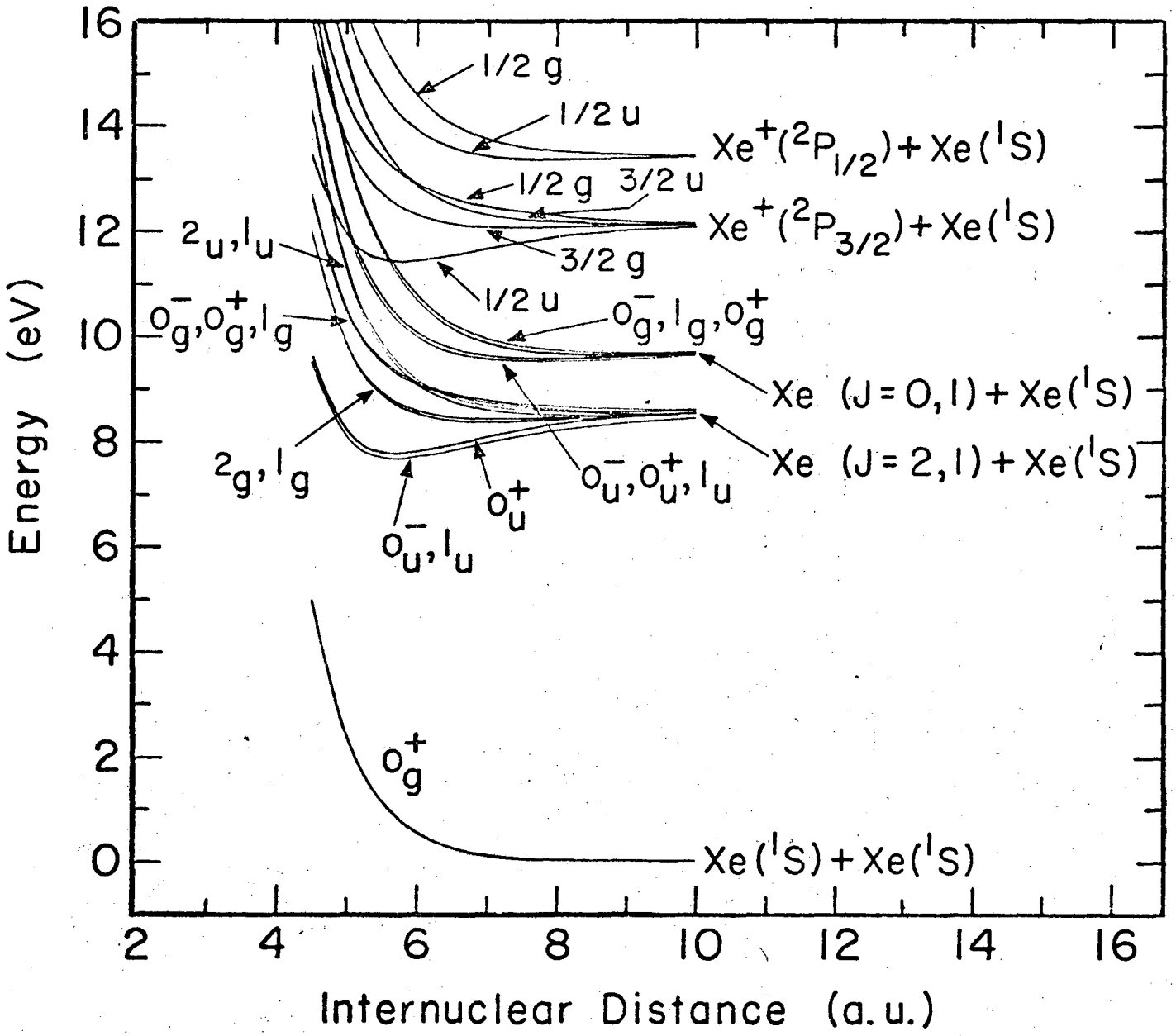
Energy (eV)
Internuclear Distance (a.u.)
1/2 g
1/2 u
Xe+(2P1/2)+Xe(1S)
1/2 g 3/2 u
Xe+(2P3/2)+Xe(1S)
2u,1u
3/2 g
1/2 u
0g−,0g+,1g
0g−,1g,0g+
Xe (J=0,1)+Xe(1S)
Xe (J=2,1)+Xe(1S)
2g,1g
0u−,0u+,1u
0u+
0u−,1u
0g+
Xe(1S)+Xe(1S)

Fig. 6

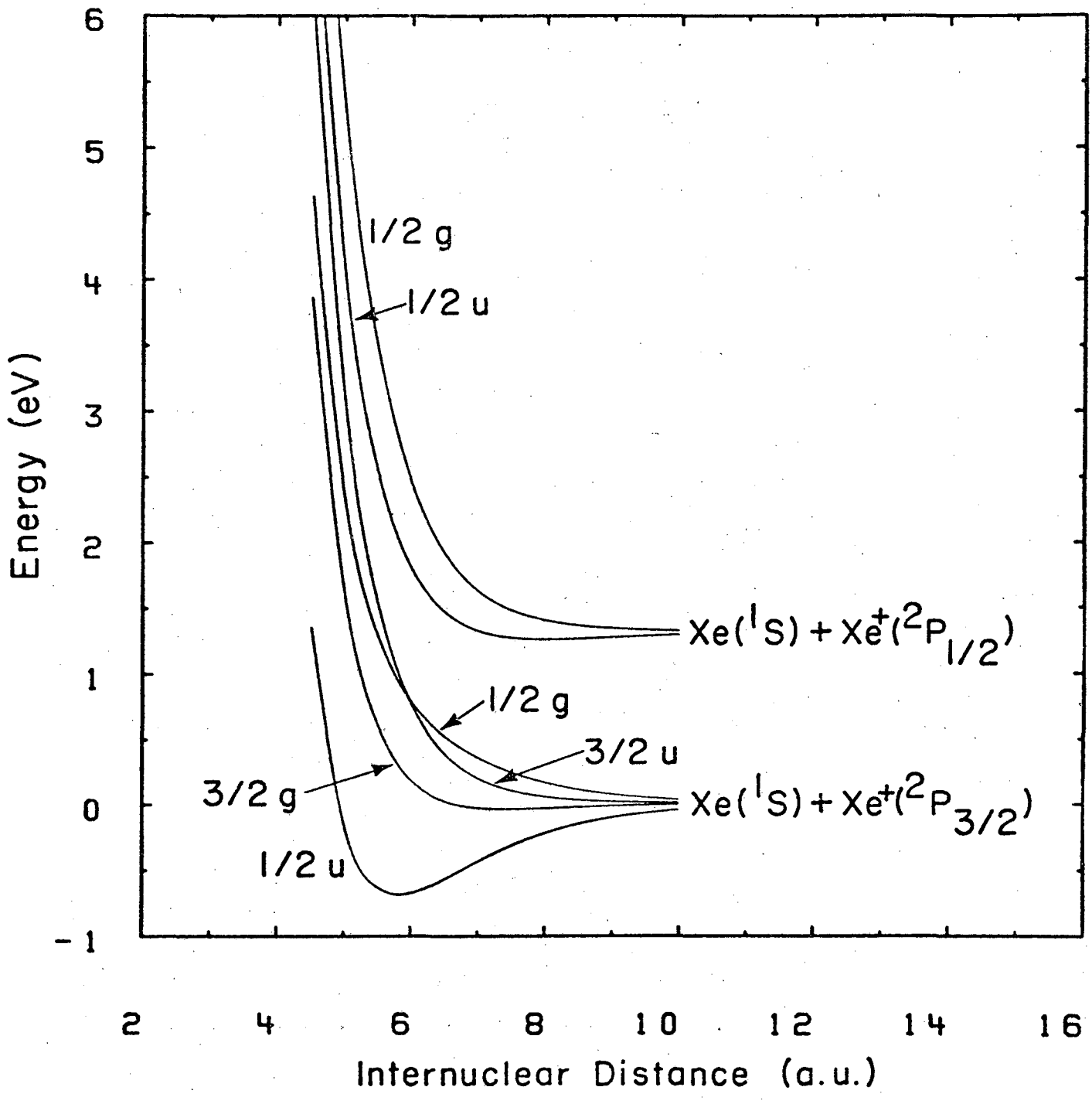
6
5
4
3
2
1
0
-1
Energy (eV)
1/2 g
1/2 u
Xe(1S) + Xe+(2P1/2)
1/2 g
3/2 u
3/2 g
Xe(1S) + Xe+(2P3/2)
1/2 u
2
4
6
8
10
12
14
16
Internuclear Distance (a.u.)

Fig. 7

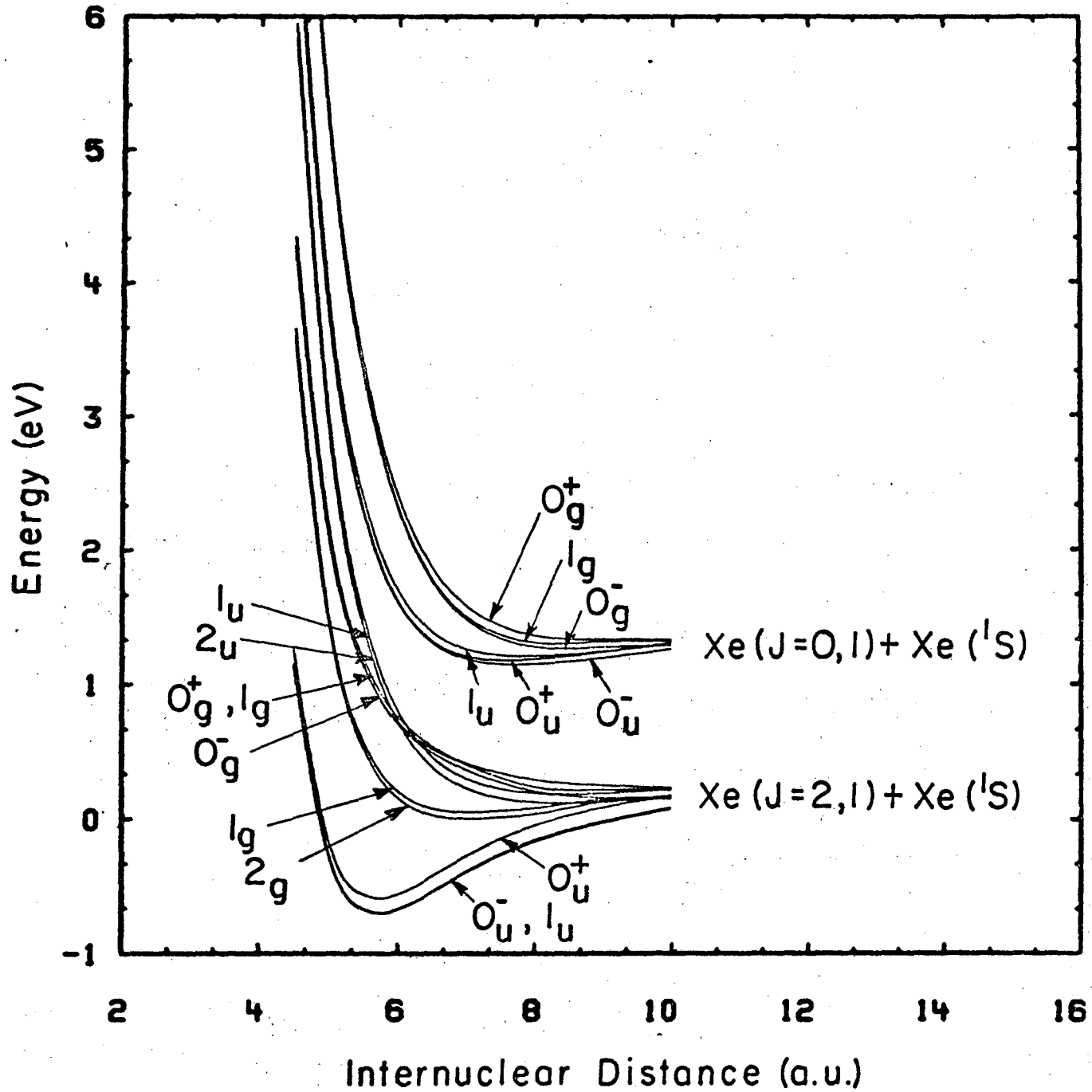
Energy (eV)
Internuclear Distance (a.u.)
Xe (J=0,1) + Xe (¹S)
Xe (J=2,1) + Xe (¹S)
$O_g^+$
$1_g$
$O_g^-$
$1_u$
$O_u^+$
$O_u^-$
$1_u$
$2_u$
$O_g^+, 1_g$
$O_g^-$
$1_g$
$2_g$
$O_u^+$
$O_u^-, 1_u$

Fig. 8

This report was done with support from the Department of Energy. Any conclusions or opinions expressed in this report represent solely those of the author(s) and not necessarily those of The Regents of the University of California, the Lawrence Berkeley Laboratory or the Department of Energy.

*TECHNICAL INFORMATION DEPARTMENT*
*LAWRENCE BERKELEY LABORATORY*
*UNIVERSITY OF CALIFORNIA*
*BERKELEY, CALIFORNIA 94720*